

RESEARCH ARTICLE

10.1002/2015JD023729

Key Points:

- Variations of CH₃Cl and N₂O in the LMS observed by CARIBIC are presented
- Stratospheric lifetime of CH₃Cl is estimated based on the correlation between CH₃Cl and N₂O
- Partitioning of stratospheric and tropical/extratropical tropospheric air in the LMS is examined

Correspondence to:

T. Umezawa,
umezawa.taku@nies.go.jp

Citation:

Umezawa, T., A. K. Baker, C. A. M. Brenninkmeijer, A. Zahn, D. E. Oram, and P. F. J. van Velthoven (2015), Methyl chloride as a tracer of tropical tropospheric air in the lowermost stratosphere inferred from IAGOS-CARIBIC passenger aircraft measurements, *J. Geophys. Res. Atmos.*, 120, 12,313–12,326, doi:10.1002/2015JD023729.

Received 2 JUN 2015

Accepted 30 OCT 2015

Accepted article online 3 NOV 2015

Published online 4 DEC 2015

Methyl chloride as a tracer of tropical tropospheric air in the lowermost stratosphere inferred from IAGOS-CARIBIC passenger aircraft measurements

T. Umezawa^{1,2}, A. K. Baker¹, C. A. M. Brenninkmeijer¹, A. Zahn³, D. E. Oram⁴, and P. F. J. van Velthoven⁵

¹Max Planck Institute for Chemistry, Mainz, Germany, ²Now at National Institute for Environmental Studies, Tsukuba, Japan, ³Institute for Meteorology and Climate Research, Karlsruhe Institute of Technology, Karlsruhe, Germany, ⁴National Centre for Atmospheric Science, Centre for Ocean and Atmospheric Sciences, School of Environmental Sciences, University of East Anglia, Norwich, UK, ⁵Royal Netherlands Meteorological Institute, De Bilt, Netherlands

Abstract We present variations of methyl chloride (CH₃Cl) and nitrous oxide (N₂O) in the lowermost stratosphere (LMS) obtained from air samples collected by the In-service Aircraft for a Global Observing System-Civil Aircraft for the Regular Investigation of the atmosphere Based on an Instrument Container (IAGOS-CARIBIC) passenger aircraft observatory for the period 2008–2012. To correct for the temporal increase of atmospheric N₂O, the CARIBIC N₂O data are expressed as deviations from the long-term trend at the northern hemispheric baseline station Mauna Loa, Hawaii (ΔN_2O). ΔN_2O undergoes a pronounced seasonal variation in the LMS with a minimum in spring. The amplitude increases going deeper in the LMS (up to potential temperature of 40 K above the thermal tropopause), as a result of the seasonally varying subsidence of air from the stratospheric overworld. Seasonal variation of CH₃Cl above the tropopause is similar in phase to that of ΔN_2O . Significant correlations are found between CH₃Cl and ΔN_2O in the LMS from winter to early summer, both being affected by mixing between stratospheric air and upper tropospheric air. This correlation, however, disappears in late summer to autumn. The slope of the CH₃Cl- ΔN_2O correlation observed in the LMS allows us to determine the stratospheric lifetime of CH₃Cl to be 35 ± 7 years. Finally, we examine the partitioning of stratospheric air and tropical/extratropical tropospheric air in the LMS based on a mass balance approach using ΔN_2O and CH₃Cl. This analysis clearly indicates efficient inflow of tropical tropospheric air into the LMS in summer and demonstrates the usefulness of CH₃Cl as a tracer of tropical tropospheric air.

1. Introduction

Methyl chloride (CH₃Cl) is a predominantly natural trace gas with its main sources considered to be vegetation [e.g., Yokouchi *et al.*, 2002] and biomass burning [e.g., Lobert *et al.*, 1999]. The global average CH₃Cl mixing ratio is ~540 ppt (parts per trillion = pmol mol⁻¹), and its global atmospheric lifetime is ~1 year being primarily determined by reaction with hydroxyl radicals (OH) in the troposphere [Carpenter *et al.*, 2014]. CH₃Cl is the dominant natural source of ozone-depleting chlorine in the stratosphere [Carpenter *et al.*, 2014; Santee *et al.*, 2013]. The local chemical lifetime of CH₃Cl in the stratosphere is much longer, enabling its use as a tracer of stratospheric dynamics [Santee *et al.*, 2013].

Nitrous oxide (N₂O) is the third most important greenhouse gas. It is also currently the ozone-depleting substance with the largest emission from human activities and is expected to remain so throughout this century [Ravishankara *et al.*, 2009]. The atmospheric N₂O mixing ratio is increasing at a rate of ~0.7 ppb yr⁻¹ due to increasing anthropogenic emissions [e.g., Prinn *et al.*, 1990; Hall *et al.*, 2007]. N₂O is photochemically destroyed in the stratosphere, giving an atmospheric lifetime of ~120 years [e.g., Volk *et al.*, 1997]. N₂O is a useful tracer to examine transport processes in the stratosphere and across the extratropical tropopause [e.g., Hegglin *et al.*, 2006; Ishijima *et al.*, 2010; Assonov *et al.*, 2013].

In the absence of a tropospheric sink, N₂O is well mixed in the troposphere and shows a clear vertical decrease in the stratosphere [Ishijima *et al.*, 2010; Santee *et al.*, 2013]. CH₃Cl also decreases with altitude in the stratosphere [Schmidt *et al.*, 1985; Santee *et al.*, 2013]. However, a particular feature of atmospheric CH₃Cl is its latitudinal gradient in the troposphere with mixing ratios peaking in the tropics due to strong

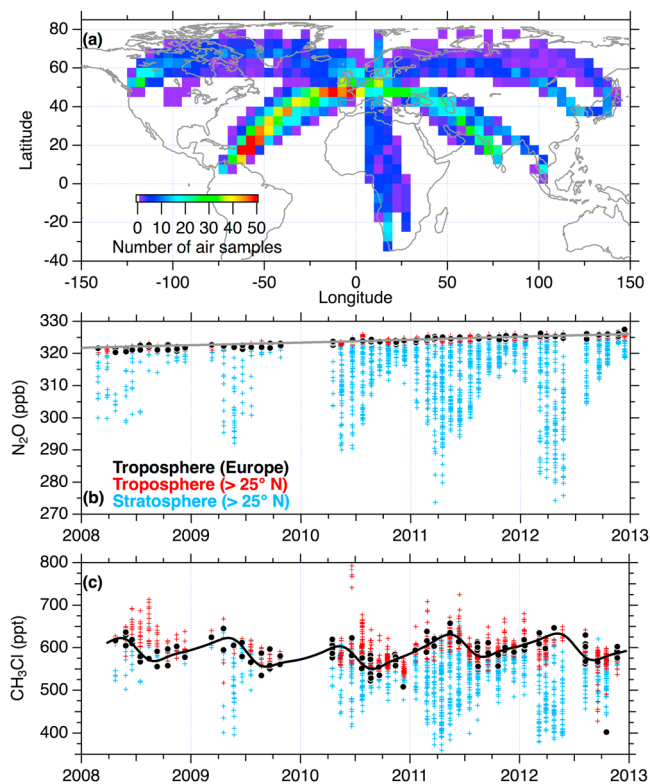


Figure 1. (a) Number of air samples collected by CARIBIC for the period 2008–2012 in 5° bins. (b) Time series of N_2O mixing ratio north of 25°N . Tropospheric and stratospheric air samples are shown by red and light blue crosses, respectively, and the tropospheric data over Europe [Umezawa *et al.*, 2014] are shown by the black circles. Stratospheric air was identified by comparing to the long-term trend deduced for the Mauna Loa (MLO) data (gray line; see text). (c) Time series of CH_3Cl mixing ratio north of 25°N . Symbols are in the same manner as Figure 1b. A best fit curve for the data over Europe (black circles) is also shown by the black line.

Based on an Instrument Container (IAGOS-CARIBIC) passenger aircraft observatory and explore their usability to distinguish air masses of stratospheric/tropospheric and tropical/extratropical tropospheric origins.

2. Experimental Methods

IAGOS-CARIBIC (In-service Aircraft for a Global Observing System-Civil Aircraft for the Regular Investigation of the atmosphere Based on an Instrument Container) is a flying observatory carrying currently 15 instruments in an air freight container (<http://www.caribic-atmospheric.com>) [Brenninkmeijer *et al.*, 2007]. Series of (typically) four intercontinental flights have been conducted almost monthly and whole air samples have been collected into two types of air collectors during flights: 2 sets of TRAC (Triggered Retrospective Air Collector) housing 14 glass flasks each and HIREs (High-Resolution Sampler) accommodating 88 steel flasks [e.g., Schuck *et al.*, 2012]. The installation of HIREs in 2010 improved the averaged sampling resolution (28 to 116 whole air samples in total for one flight series). The number of air samples in each 5° longitude and latitude bin for the period April 2008 to December 2012 is presented in Figure 1a. The air samples have been analyzed for CH_3Cl in the laboratory by using a gas chromatograph coupled with mass spectrometry (GC-MS) at the University of East Anglia (UEA) since May 2005 [Leedham Elvidge *et al.*, 2015] and a gas chromatograph with flame ionization detection (GC-FID) at the Max Planck Institute for Chemistry (MPIC) since April 2008 [Baker *et al.*, 2010]. For data analyses in this study, we use the MPIC CH_3Cl data analyzed by GC-FID (plotted in Figure 1) because of their higher density for the tropopause region. Overall uncertainty of the MPIC measurements is 6% and mixing ratios reported in this study are referenced to the NOAA CH_3Cl scale [Montzka *et al.*, 2011]. An offset of 23 ppt (the MPIC measurements are lower) is taken into account based

tropical emissions [Yokouchi *et al.*, 2000; Santee *et al.*, 2013; Umezawa *et al.*, 2014]. As a consequence, CH_3Cl is a potentially useful tracer of tropical tropospheric air in the upper troposphere/lowermost stratosphere (UT/LMS) [Scheeren *et al.*, 2003], but this topic has remained unexamined due to limited availability of CH_3Cl data.

Since air traffic at northern midlatitudes primarily takes place in the UT/LMS, measurements onboard commercial airliners are useful for studying the budget of trace gases and aerosols in the UT/LMS, stratosphere-troposphere exchange and the related processes [e.g., Thouret *et al.*, 2006; Sawa *et al.*, 2008; Zahn *et al.*, 2014]. Although commercial aircraft cruise within a narrow range of pressures (200–300 hPa), the local tropopause height varies with season, depends on latitude, and is affected by actual synoptic conditions. As a consequence, passenger aircraft have opportunities to scan the UT/LMS in a vertical sense at altitudes of effectively up to ~ 5 km above the tropopause. In this study, we present extensive CH_3Cl and N_2O measurements in the UT/LMS from air samples collected by the In-service Aircraft for a Global Observing System-Civil Aircraft for the Regular Investigation of the atmosphere

on intercomparisons with UEA whose measurements are referenced to the NOAA CH₃Cl scale [see *Umezawa et al.*, 2014]. The offset value is comparable to interlaboratory differences found in an intercomparison experiment [Hall et al., 2014]. N₂O mixing ratios in the CARIBIC air samples were analyzed by a gas chromatograph equipped with electron capture detection (GC-ECD) with a precision of 0.15% (<0.5 ppb) [Schuck et al., 2009], and the N₂O data are reported on the NOAA-2006 N₂O scale [Hall et al., 2007]. For contrast, this study presents analysis of the LMS data, whereas *Umezawa et al.* [2014] focused on variations in the UT; we however note that both studies explore the CH₃Cl and N₂O data sets obtained by the ongoing CARIBIC project.

3. Data Analysis

3.1. ΔN₂O and Identification of LMS Air Samples

N₂O mixing ratios in the CARIBIC air samples are used to identify stratospheric air [Umezawa et al., 2014]. The method is conceptually similar to that applied by *Assonov et al.* [2013]. In the present study, the CARIBIC N₂O data north of 25° N were compared with the long-term trend observed at Mauna Loa (MLO, gray line in Figure 1b), Hawaii (<ftp://ftp.cmdl.noaa.gov/hats/n2o/>) [Hall et al., 2007], which was deduced by applying a digital filtering technique [Nakazawa et al., 1997]. The deviation of N₂O mixing ratios in CARIBIC air samples from the MLO trend (ΔN₂O) represents the depletion in N₂O relative to northern hemispheric baseline air. The main purpose is to correct N₂O data taken in different years for the near-linear increasing trend of atmospheric N₂O. If ΔN₂O was more than 1.3 ppb (2 standard deviations of the MLO data) below the MLO trend, the air sample was classified as stratospheric. Accordingly, all the CARIBIC air samples were classified into either stratospheric (light blue in Figure 1b) or tropospheric (red and black in Figure 1b) air. For the observation period (April 2008 to December 2012), we identified 1474 stratospheric air samples among 3716 air samples in total. We note that the N₂O-based tropopause is similar to the O₃-based chemical tropopause [Zahn and Brenninkmeijer, 2003; Thouret et al., 2006], which we used when N₂O data were not available (only one sample in this study). We prefer the use of N₂O over that of O₃ because N₂O and CH₃Cl are analyzed for the same air samples. A comparison between the N₂O-based tropopause and the dynamical tropopause will be presented in section 4.5.

Two factors contribute to the vertical decrease of N₂O in the stratosphere. First, major photochemical loss of N₂O occurs in the middle stratosphere (~30 km) [e.g., Ishijima et al., 2010]. Second, since atmospheric N₂O increases in time, the older (aged) air in the stratosphere is lower in N₂O. As described above, we use ΔN₂O, but the method is applied uniformly for all data with different air ages, and thus, this age effect is not taken into account in this study. We however consider that the chemical sink effect is the dominant controlling factor of the variability seen in this study. Given that the present N₂O increase rate is ~0.7 ppb yr⁻¹ [e.g., Hall et al., 2007], the age effect corresponds to less than ~2 ppb, based on the ages of air as deduced from the CARIBIC SF₆ measurements being less than 3 years in the LMS (not shown in this paper). We note that the age of air calculated from the CARIBIC data is in agreement with previous estimates when compared in layers with corresponding ΔN₂O [Engel et al., 2002] and in corresponding ϕ-Θ space (described in section 3.3) [Bönisch et al., 2009].

3.2. Meteorological Data

The meteorological analyses for CARIBIC are based on the European Centre for Medium-Range Weather Forecasting (ECMWF) meteorological data with a horizontal resolution of 1° in latitude and longitude at 6 h time intervals. The ECMWF data were interpolated linearly for positions and time along the CARIBIC aircraft flight tracks [van Velthoven, 2015]. Potential temperature (Θ), potential temperature at the thermal tropopause (Θ_{TP}), potential vorticity (PV), equivalent latitude (ϕ), and backward trajectories are calculated from the ECMWF data. The interpolation scheme for the ECMWF data demonstrated excellent agreement between retrieved and measured temperature of -0.45 ± 1.2 K [Dyrov et al., 2014]. For the equivalent latitude potential temperature (ϕ-Θ) coordinate plots (described later), we use the potential temperature measured onboard.

3.3. Vertical and Latitudinal Coordinates

To present vertical distributions of ΔN₂O and CH₃Cl, we use potential temperature with respect to the thermal tropopause ($\Delta\Theta_{TP} = \Theta - \Theta_{TP}$). It has been shown that the use of ΔΘ_{TP} as a vertical coordinate corrects for variations of potential temperature at the tropopause, giving significantly improved compactness of trace gas profiles in the tropopause region [Hoor et al., 2004; Sawa et al., 2008]. It should be noted that these two studies

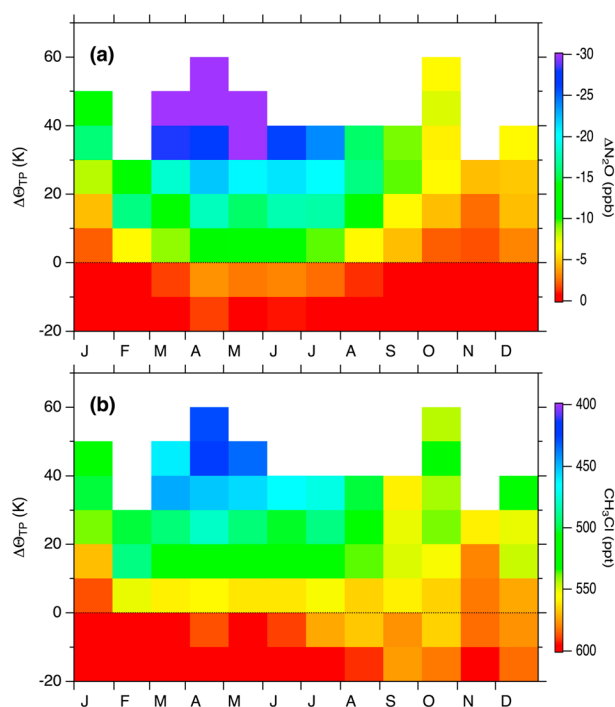


Figure 2. Seasonal variations of (a) ΔN_2O and (b) CH_3Cl at different potential temperature layers with respect to the thermal tropopause ($\Delta\Theta_{TP}$) in the UT/LMS observed by CARIBIC. The CARIBIC data north of $25^\circ N$ were analyzed. Each bin in color has more than five data points.

under diabatic processes, the φ - Θ coordinate system works exclusively for conditions dominated by adiabatic air parcel motion. *Manney et al.* [2011] indicated that the φ - Θ coordinate system could obscure fine structures of trace gas distributions around a jet. *Pan et al.* [2012] showed that the φ - Θ coordinate system does not work equally in the UT and the LMS and at all latitudes, due to the steep gradients of Θ isentropes in the subtropics. We note that the low-latitude data presented in this study are obtained only in the UT, that is, the low-latitude data are correctly allocated to the troposphere in the φ - Θ coordinate system, but φ gives a realistic value only in the region adjacent to the tropopause where a significant gradient of the PV-defined φ still exists. In this study, we examine global climatological distributions of N_2O and CH_3Cl in the LMS and use of the φ - Θ coordinate system suits this purpose even given its aforementioned limitations.

4. Results and Discussion

4.1. Time Series of N_2O and CH_3Cl in the UT/LMS

Figure 1b shows time series of N_2O observed by CARIBIC for 2008–2012. We highlight data over Europe where CARIBIC has the highest data density to depict a continuous time series in the UT [*Umezawa et al.*, 2014]. A near-linear increase of the N_2O mixing ratio is visible in the UT over Europe (black circles) with no significant seasonality over the years. The observed N_2O increase is in good agreement with the long-term trend at MLO (gray line). In contrast, the stratospheric samples north of $25^\circ N$ (light blue crosses) show clear depletions in N_2O especially in spring when the CARIBIC aircraft frequently encounters deeper stratospheric air. It is also noted that the installation of an additional air sampler in 2010 (see section 2) increased the sample density considerably. The increased number of stratospheric samples since then is also due to the CARIBIC aircraft flying more frequently at higher northern latitudes because of changes in flight destinations [see also *Umezawa et al.*, 2014]. The CH_3Cl mixing ratio in the UT over Europe observed by CARIBIC (black circles with a black line in Figure 1c) varies with clear seasonality and without significant interannual variations [*Umezawa et al.*, 2014]. In general, stratospheric samples are lower in CH_3Cl , showing a curtain-like seasonal pattern similar to N_2O .

used the dynamical tropopause at 2 PVU ($1 \text{ PVU} = 10^{-6} \text{ K m}^2 \text{ kg}^{-1} \text{ s}^{-1}$) to calculate $\Delta\Theta_{TP}$, being different from this study in which we use the thermal tropopause defined by the World Meteorological Organization [WMO, 1957]. The WMO thermal tropopause at midlatitudes on average coincides with the 3.5 PVU isosurface in the extratropics [*Hoerling et al.*, 1991] and is thus at higher altitudes than the 2 PVU isosurface.

We also use an equivalent latitude (φ) and potential temperature (Θ) coordinate system to better present climatological distributions. Equivalent latitude is calculated based on the area enclosed by the specific PV contour on a given isentrope. Previous studies demonstrated that the illustration of data in a φ - Θ coordinate system effectively removes trace gas variations in the extratropical LMS due to synoptic (Rossby-wave driven) meridional excursions of the jet streams [*Hoor et al.*, 2004; *Sawa et al.*, 2008; *Bönisch et al.*, 2009]. Since PV is not conserved

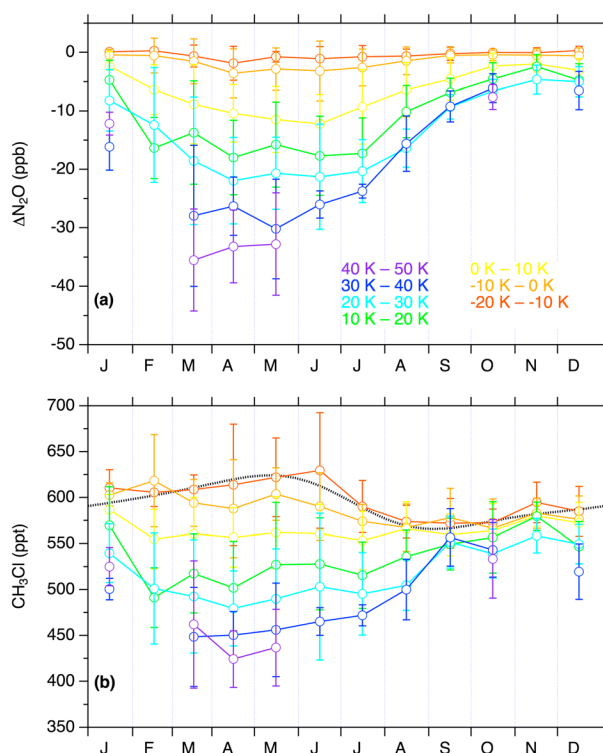


Figure 3. Seasonal variations of (a) $\Delta\text{N}_2\text{O}$ and (b) CH_3Cl at different $\Delta\Theta_{\text{TP}}$ layers (shown by different colors). Also shown in Figure 3b is the best fit curve deduced for the UT data over Europe. As in Figure 2, the CARIBIC data north of 25°N were analyzed and only bins with more than five data points are shown.

subsiding from the stratospheric overworld during winter-spring measurably leaks across the tropopause shaping a small seasonal depletion even below $\Delta\Theta_{\text{TP}} = 0$ in April–July (Figures 2a and 3a). The largest vertical gradient of $\Delta\text{N}_2\text{O}$ in the LMS occurs in spring (March–May) with an almost linear decrease of $-0.58 \pm 0.09 \text{ ppb K}^{-1}$ (Figure 4a). In the subsequent months, the vertical gradient of $\Delta\text{N}_2\text{O}$ in the LMS lessens and reaches its seasonal minimum of $-0.11 \pm 0.06 \text{ ppb K}^{-1}$ for October–December.

Turning our attention to seasonal variations of CH_3Cl in the LMS, we see a similarity with $\Delta\text{N}_2\text{O}$ (Figure 2b), namely, a spring minimum and an autumn maximum. In the high layer ($30 \text{ K} < \Delta\Theta_{\text{TP}} \leq 40 \text{ K}$), the minimum and maximum are found to be $425 \pm 54 \text{ ppt}$ in March and $534 \pm 31 \text{ ppt}$ in September (Figure 3b). In analogy with $\Delta\text{N}_2\text{O}$, the vertical gradient of CH_3Cl in the LMS peaks in spring ($-2.8 \pm 0.7 \text{ ppt K}^{-1}$ in March–May), and CH_3Cl in the LMS forms an almost uniform profile ($-0.5 \pm 0.2 \text{ ppt K}^{-1}$) in October (Figure 4b). In contrast to the LMS profiles, in the UT, a seasonal variation with a late summertime minimum is observed [Umezawa *et al.*, 2014], which is opposite in phase to the LMS. As a result of the different seasonal variations in the LMS and UT, the vertical profiles of CH_3Cl in spring and autumn intersect each other around the tropopause (Figure 4).

It has been shown that N_2O mixing ratios in the stratosphere represent well the age of stratospheric air [e.g., Andrews *et al.*, 2001; Waugh and Hall, 2002], and the observed seasonal variations of $\Delta\text{N}_2\text{O}$ are attributable to the seasonally varying descent of air from the stratospheric overworld [e.g., Appenzeller *et al.*, 1996]. As described above, the springtime minima of $\Delta\text{N}_2\text{O}$ and CH_3Cl in the LMS are well in phase, indicating that these minima are governed by stratospheric dynamics, i.e., the downward branch of the Brewer-Dobson circulation bringing aged stratospheric air depleted in N_2O and CH_3Cl . This is consistent with the expectation that long-lived tracers shape the same patterns of isolines in the stratosphere [Plumb and Ko, 1992]. Indeed, distributions of CH_3Cl and N_2O reported by satellite observations that cover up to the middle stratosphere showed similar spatial patterns [Santee *et al.*, 2013]. However, as described above, CH_3Cl in the LMS varies somewhat differently from $\Delta\text{N}_2\text{O}$ in summer-autumn. CH_3Cl at layers $\Delta\Theta_{\text{TP}} > 20 \text{ K}$ in the LMS

4.2. Seasonal and Vertical Variations of $\Delta\text{N}_2\text{O}$ and CH_3Cl

Overviews of vertical gradients and seasonal variations of $\Delta\text{N}_2\text{O}$ and CH_3Cl are illustrated using $\Delta\Theta_{\text{TP}}$ as a vertical coordinate (Figure 2). As clearly seen in this figure, $\Delta\text{N}_2\text{O}$ undergoes pronounced seasonal variations in the LMS ($\Delta\Theta_{\text{TP}} > 0$) with a minimum in spring, while it reaches a maximum in autumn. The seasonal $\Delta\text{N}_2\text{O}$ variations in the respective $\Delta\Theta_{\text{TP}}$ layers are plotted in Figure 3, which shows that the amplitude of the seasonal $\Delta\text{N}_2\text{O}$ variation increases going deeper into the LMS (i.e., upward from the tropopause). For instance, in the highest $\Delta\Theta_{\text{TP}}$ layer that the CARIBIC aircraft covers most of the year ($30 \text{ K} < \Delta\Theta_{\text{TP}} \leq 40 \text{ K}$), $\Delta\text{N}_2\text{O}$ minimizes at $-30.2 \pm 8.5 \text{ ppb}$ in May and reaches a maximum of $-6.1 \pm 2.4 \text{ ppb}$ in October. In contrast, no significant seasonal variation of $\Delta\text{N}_2\text{O}$ is observed in the UT ($\Delta\Theta_{\text{TP}} < 0$), which gives the annual average and the standard deviation of $+0.17$ and 0.65 ppb , respectively. It is apparent that air

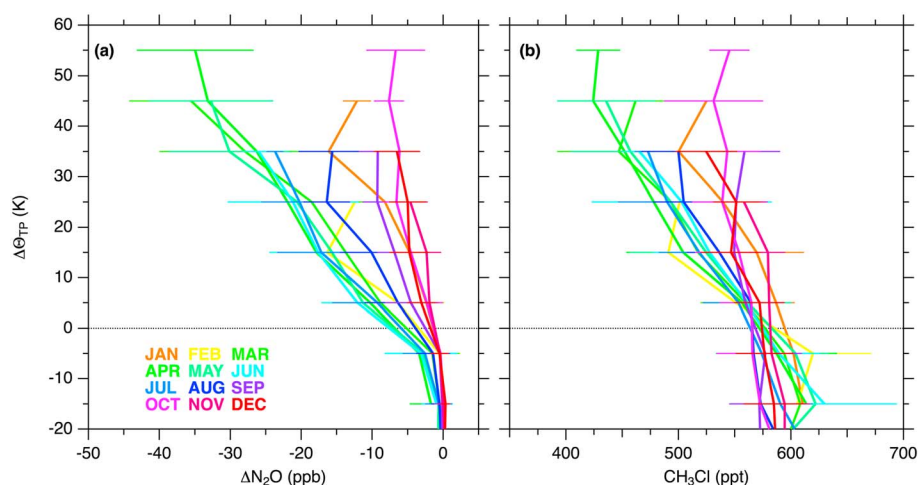


Figure 4. Vertical profiles of (a) $\Delta\text{N}_2\text{O}$ and (b) CH_3Cl as a function of $\Delta\Theta_{\text{TP}}$ in each month (colored). Error bars represent standard deviations within the respective $\Delta\Theta_{\text{TP}}$ bins. As in Figure 2, the CARIBIC data north of 25°N were analyzed and only bins with more than five data points are shown.

reaches its maximum ~ 1 month earlier (September) than $\Delta\text{N}_2\text{O}$ (Figures 2b and 3b), and the difference could be attributable to signals from the troposphere. In the following sections, we will argue that CH_3Cl variations to a degree reflect transport of air from the tropical UT into the LMS.

It is also noteworthy that, in some months, the vertical profiles of $\Delta\text{N}_2\text{O}$ and CH_3Cl have apparent “kinks” (rapid changes in the vertical gradients in Figure 4). This likely represents the presence of a transition layer, which is partly tropospheric and partly stratospheric in chemical characteristics, i.e., the extratropical transition layer (ExTL), as empirically characterized based on aircraft and satellite data of CO , O_3 , H_2O , and CO_2 [Hoor et al., 2004; Pan et al., 2004; Sawa et al., 2008; Hegglin et al., 2009]. Consistent with these studies, such a sharp change in vertical gradient can be found more clearly in the CARIBIC CO (not shown) and acetone [Sprung and Zahn, 2010] data, and the kinks observed for $\Delta\text{N}_2\text{O}$ and CH_3Cl are coincident with those of CO when discernible. It is noteworthy that the phenomenon is seen here for $\Delta\text{N}_2\text{O}$ and CH_3Cl , although shorter-lived trace gases (e.g., CO and acetone) can reflect mixing with tropospheric air occurring over shorter timescales [Sprung and Zahn, 2010; Gettelman et al., 2011].

4.3. Correlations Between CH_3Cl and $\Delta\text{N}_2\text{O}$

In the stratosphere, two long-lived tracers (local chemical lifetimes being distinctly longer than transport timescales) form compact linear relations under the assumption of slope equilibrium (faster quasi-horizontal versus vertical transport in absence of sources and sinks) [Plumb and Ko, 1992]. Waugh et al. [1997] further pointed out that an anomalous mixing line connecting reservoirs of different chemical lifetimes may lead to a curved correlation of the two tracers. The concept of mixing lines on a tracer-tracer scatterplot has been also applied for identifying the ExTL in which air composition is a mixture of stratospheric and tropospheric air [e.g., Hoor et al., 2002]. Given that both N_2O and CH_3Cl are long-lived compared to timescales of transport processes in the UT/LMS, the correlation of $\Delta\text{N}_2\text{O}$ and CH_3Cl in the LMS is determined by mixing of the reservoirs “LMS air” and “tropospheric air” and effective horizontal mixing within the LMS.

Figure 5 presents CH_3Cl - $\Delta\text{N}_2\text{O}$ scatterplots for different seasons along with the number of data points shown as colors of individual bins. The correlation plots exhibit a fair amount of scatter, but to a large extent, they can be considered to represent climatological distributions by virtue of the fact that they include multiple years of CARIBIC measurements in the LMS. During December–February (DJF), March–May (MAM), and June–August (JJA), we find linear relationships between CH_3Cl and $\Delta\text{N}_2\text{O}$ in the LMS with significant correlation coefficients ($R^2 > 0.60$). In particular, in spring (MAM) when the wintertime downward mass transport accumulates aged stratospheric air in the LMS [Appenzeller et al., 1996], the scatterplot reaches the lowest $\Delta\text{N}_2\text{O}$ and CH_3Cl values with a slope of the correlation of $5.77 \pm 0.15 \text{ ppt ppb}^{-1}$ (Figure 5b). In the following season (JJA), the slope remains almost the same ($5.76 \pm 0.15 \text{ ppt ppb}^{-1}$) (Figure 5c). In this respect, the vertical gradients of $\Delta\text{N}_2\text{O}$ and CH_3Cl in JJA remain the same as those in MAM (Figures 2 and 4). However, during

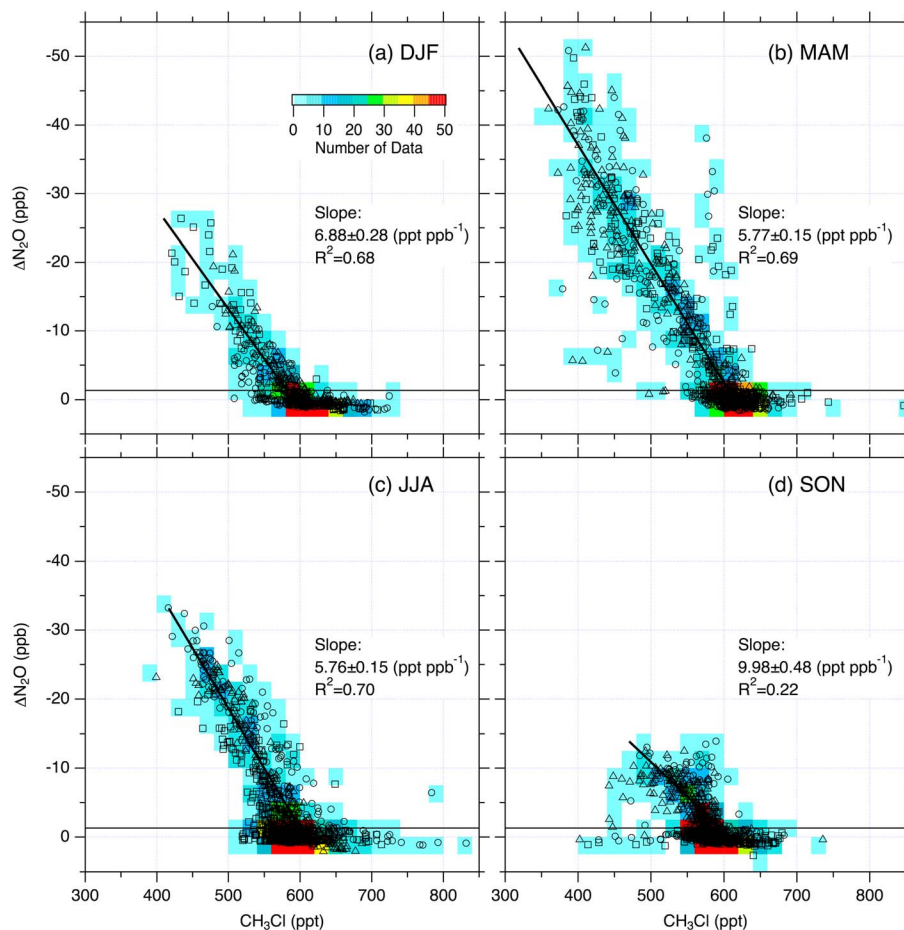


Figure 5. Scatterplots of CH₃Cl as a function of ΔN₂O for (a) December–February (DJF), (b) March–May (MAM), (c) June–August (JJA), and (d) September–November (SON). Data in the first, second, and third months are shown by circles, triangles, and squares, respectively. Geometric mean regression lines for the stratospheric data and their slopes with errors of 67% confidence intervals are also shown. Colors of individual bins (2.5 ppb in ΔN₂O × 20 ppt in CH₃Cl) indicate the number of the CARIBIC data points. The horizontal solid lines show the N₂O-based tropopause. We also examined a bootstrap method with 1000 iterations to confirm robustness of the regression slopes, obtaining insignificantly different values.

August (late JJA), the LMS data are distributed closer to the N₂O-based tropopause than in the preceding 2 months and slightly lose compactness of the correlation, eventually forming the collapsed linear relations in autumn (September–November, SON) (Figure 5d).

4.4. Stratospheric Lifetime of CH₃Cl

In this section, we estimate the stratospheric lifetime of CH₃Cl based on the slope of the correlation plot between ΔN₂O and CH₃Cl in the LMS, before examining quantification of air mass origins (discussed in the next section). From the viewpoint of ozone destruction, the stratospheric lifetime represents how rapidly the reactive degradation product is released. The impact of a chemical on stratospheric ozone (i.e., the ozone-depleting potential or ODP) is proportional to the total atmospheric lifetime [e.g., Solomon et al., 1992]. The stratospheric lifetime is part of the total atmospheric lifetime, which is a prime factor determining abundance of an atmospheric compound given global emissions [e.g., Carpenter et al., 2014].

Stratospheric lifetimes of two long-lived trace gases are related as follows [Plumb and Ko, 1992]:

$$\frac{\tau_1}{\tau_2} \cong \frac{\sigma_1/\sigma_2}{d\sigma_1/d\sigma_2}, \tag{1}$$

where τ_i and σ_i are the lifetime and the average mixing ratio at steady state for a specie i and $d\sigma_1/d\sigma_2$ is a slope of the correlation at the tropopause.

For σ_1 , we applied the global surface average values in 2010: 323.1 ± 0.1 ppb for N_2O (<http://ds.data.jma.go.jp/gmd/wdcgg/pub/global/globalmean.html>) and 541 ± 2 ppt for CH_3Cl (based on the NOAA data [Montzka et al., 2011]). Plumb and Ko [1992] proposed to assume values at the tropopause for σ_1/σ_2 to represent the troposphere, but the later studies more rigorously calculated the global average (not only in the troposphere) mixing ratios [Volk et al., 1997; Brown et al., 2013]. Comparisons with the global average CH_3Cl and N_2O values calculated by Brown et al. [2013] indicate that σ_1/σ_2 could change by $< 10\%$ by approximating the global average with the surface average. We therefore consider that use of the surface average values is a practical approximation, given the larger uncertainties stemming from other factors (discussed below).

We use the slope $d\sigma_1/d\sigma_2 = 5.77 \pm 0.15$ ppt/ppb for the LMS data in MAM because the correlation in this part of the year is entirely governed by mixing with aged stratospheric air that has subsided [Bönisch et al., 2009] and is negligibly affected by recent in-mixing around the subtropical jet. We do not correct the slope for species' growth rates [Volk et al., 1997; Brown et al., 2013], since the $\Delta\text{N}_2\text{O}$ data we use have already been corrected for the trend, and since for CH_3Cl , no significant long-term trend has been observed over the observation period [Montzka et al., 2011; Umezawa et al., 2014]. Previous studies estimated slopes at the tropopause by extrapolating those calculated from subsets of the data obtained just above the tropopause [Volk et al., 1997; Laube et al., 2013; Brown et al., 2013]. We also applied this method to our $\text{CH}_3\text{Cl}-\Delta\text{N}_2\text{O}$ relationships (not shown), but, due to the scatter of the CARIBIC data, the result indicated a slope value insignificantly different from that simply deduced from the regression for the entire LMS data set (Figure 5). We therefore consider that the average slope obtained for the LMS data described above is the best available estimate at present. We note that our passenger aircraft data cover multiple years but are restricted to air approximately up to ~ 5 km above the tropopause, whereas the above cited studies used campaign data up to higher altitudes obtained by high-altitude research aircraft [Volk et al., 1997; Laube et al., 2013] or satellite data with large geographical coverage but relatively large uncertainty [Brown et al., 2013].

Given the lifetime estimate of N_2O of 122 ± 24 years [Volk et al., 1997], we calculate the lifetime of CH_3Cl to be 35 ± 7 years. To our knowledge, only Brown et al. [2013] calculated an observation-based stratospheric CH_3Cl lifetime. They arrive in the same manner at 69^{+65}_{-23} years but use satellite observations. Their lifetime estimate is twice ours, although their uncertainties are large. Based on the value by Brown et al. [2013]; SPARC [2013] assessed the best estimate of the empirical stratospheric lifetime of CH_3Cl to be 83 (28– ∞) years, while a model-based stratospheric lifetime in SPARC [2013] was 30.4 years. The total atmospheric lifetime of CH_3Cl , including the partial stratospheric lifetime, is currently assessed to be 0.9 year based on the model-derived stratospheric lifetime value of 30.4 years [Carpenter et al., 2014], which is now supported by our observation-based estimate. To support our estimate, we also calculated stratospheric lifetimes of other trace gases measured by CARIBIC in the same way, resulting in, e.g., 143 ± 28 years for CH_4 and 57 ± 14 for CFC-11. The calculated lifetime for CH_4 falls between previous estimates of 93 ± 18 years [Volk et al., 1997] and of 195^{+75}_{-42} [Brown et al., 2013] and that for CFC-11 is in good agreement with the current estimate of 52 (43–67) years [SPARC, 2013; Carpenter et al., 2014].

4.5. Seasonal Change in the Fraction of Tropical Tropospheric Air in the LMS

The LMS is the extratropical transition region between the troposphere and stratosphere and thus subject to dynamical and chemical influences of the troposphere and the stratospheric overworld. Previous studies [e.g., Ray et al., 1999; Hoor et al., 2002; Hegglin et al., 2006; Bönisch et al., 2009; Zahn et al., 2014] show that the LMS changes its chemical composition with season. In this section, we apply a mass balance method to the $\Delta\text{N}_2\text{O}$ and CH_3Cl data to quantify fractions of air of different origins in the LMS and discuss the merits of the two tracers.

In Figure 6, distributions of $\Delta\text{N}_2\text{O}$ (Figures 6a–6d) and CH_3Cl (Figures 6e–6h) obtained by CARIBIC are presented on a $\varphi-\Theta$ coordinate system for different seasons. PV isolines of 2, 4, 6, and 8 PVU are also shown (black lines). $\Delta\text{N}_2\text{O}$ is well mixed in the troposphere and shows a sharp gradient around the tropopause, with lower values in the LMS throughout the year. Clearly visible is the subsidence of N_2O -depleted stratospheric air with correspondingly higher ages of up to ~ 2.5 years in spring. In contrast, in the LMS, highest $\Delta\text{N}_2\text{O}$ values are sampled in autumn, which reflects the efficient in-mixing of N_2O -rich tropospheric air, a process named “flushing of the LMS” [Hegglin and Shepherd, 2007; Bönisch et al., 2009]. The contours of $\Delta\text{N}_2\text{O}$ lie almost in parallel to the PV isolines as were observed in the SPURT campaigns [Engel et al., 2006]. In general,

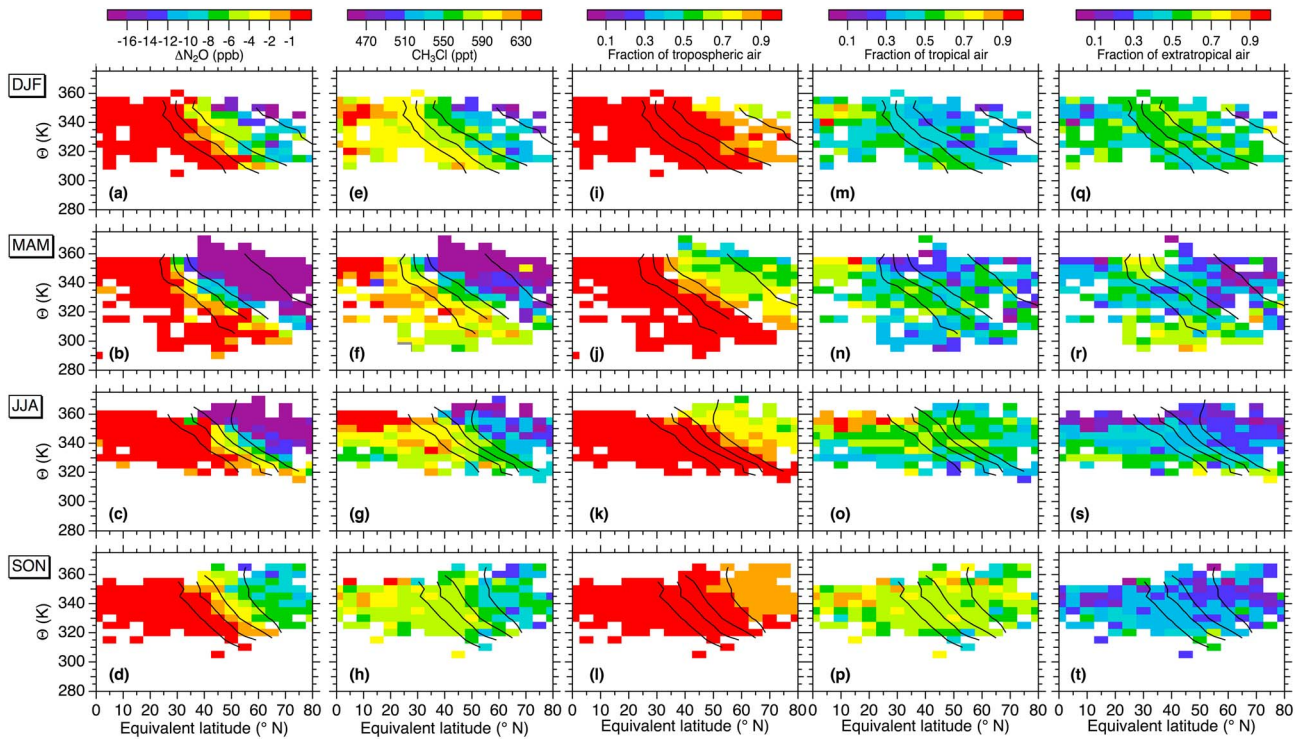


Figure 6. Equivalent latitude potential temperature ($\varphi-\Theta$) cross sections of ΔN_2O , CH_3Cl , fraction of tropospheric air based on ΔN_2O , fractions of tropical UT air, and extratropical surface air based on CH_3Cl (from left to right) for different seasons (DJF, MAM, JJA, and SON). Sets of solutions with unreasonable fraction values (e.g., below 0 or above 1) in a few bins are omitted (middle to right). Black lines show PV isolines (PV = 2, 4, 6, and 8 PVU). Note that the N_2O -based tropopause ($\Delta N_2O = -1.3$ ppb) is represented by orange in Figures 6a–6d.

the N_2O -based tropopause defined in this study ($\Delta N_2O = -1.3$ ppb colored in orange) is located between the 2 and 4 PVU isolines year round; for comparison the thermal tropopause generally lies near 3.5 PVU as mentioned earlier.

CH_3Cl is high in the tropical troposphere and decreases going deeper in the stratosphere. At first glance, the distributions of ΔN_2O and CH_3Cl are very similar. Indeed, the decrease of CH_3Cl in the LMS is similar to that of ΔN_2O in DJF and MAM; the CH_3Cl contours are distributed almost in parallel to the PV isolines and the gradient between the UT and LMS is large. However, for JJA, the gradient of CH_3Cl with PV becomes unclear (importantly in contrast to ΔN_2O), and the CH_3Cl contours obviously extend across the PV isolines on the isentropic surfaces around $\Theta = 340$ K. This feature becomes less distinct in SON, but the overall CH_3Cl level in the LMS becomes elevated and the CH_3Cl gradient across the tropopause is smallest in this season as observed in ΔN_2O . Similar features have been observed in CO_2 data also obtained by passenger aircraft [Sawa *et al.*, 2008] and can be interpreted in terms of meridional air transport on isentropic surfaces from the tropical UT to the LMS in summer to autumn [Chen, 1995; Berthet *et al.*, 2007; Sawa *et al.*, 2008; Bönisch *et al.*, 2009]. Beyond this, we claim that CH_3Cl in the LMS is disproportionately high in summer-autumn compared to other tracers and that the isopleths do not run in parallel to the tropopause.

In order to quantify fractions of tropospheric and stratospheric air in the LMS, we utilize ΔN_2O according to the mass balance equation:

$$[\Delta N_2O] = \alpha_{trop}[\Delta N_2O]_{trop} + \alpha_{strat}[\Delta N_2O]_{strat}, \tag{2}$$

$$\alpha_{trop} + \alpha_{strat} = 1, \tag{3}$$

where the square brackets represent mixing ratio, α is the tropospheric/stratospheric fraction, and subscripts “trop” and “strat” specify the troposphere and stratosphere, respectively. This concept has been applied before [Ray *et al.*, 1999; Bönisch *et al.*, 2009]. We assume $[\Delta N_2O]_{trop} = 0$ ppb (recall that $\Delta N_2O = 0$ represents northern hemispheric baseline air, i.e., the long-term trend at MLO). $[\Delta N_2O]_{strat}$ should be defined as the value at the upper boundary of the LMS ($\Theta = 380$ K) or in the overworld. Bönisch *et al.* [2009] fixed the

mean age of air to be 3 years as the upper boundary in a similar mass balance method. The 3 year mean age of air is translated to approximately $\Delta N_2O = -70$ ppb according to polynomial relationships between N_2O and mean age of air in the stratosphere [Andrews *et al.*, 2001; Engel *et al.*, 2002]. We accordingly set $[\Delta N_2O]_{\text{strat}} = -70$ ppb. From the SPURT campaigns [Engel *et al.*, 2006], an N_2O mixing ratio of 263.2 ppb at $\Theta = 378.2$ was observed in April 2003, which corresponds to $\Delta N_2O = -54.8$ ppb. Werner *et al.* [2010] also reported N_2O data obtained by using high-altitude aircraft, in which ΔN_2O reached approximately down to -60 ppb outside the Arctic vortex. These previous measurements imply that our upper boundary is located somewhat above 380 K isopleth, being consistent with Bönisch *et al.* [2009]. We note that, with the above boundary conditions, the N_2O -based tropopause (-1.3 ppb) defined in this study corresponds to $\alpha_{\text{trop}} = 0.98$.

Equations (2) and (3) are then solved for α_{trop} in each φ - Θ bin, and the result is shown in Figures 6i–6l. The lowest α_{trop} is found in spring (MAM) with values reaching down to below 0.4 above the 6 PVU isoline. On the other hand, in SON, the α_{trop} value exceeds 0.8 in the entire LMS, including the polar region. Using mean ages calculated from CO_2 and SF_6 , Bönisch *et al.* [2009] also estimated the seasonal change of α_{trop} , which is consistent in spatial pattern and numbers with this study. Ray *et al.* [1999] also estimated the fraction of tropospheric/stratospheric air based on balloon measurements of CFC-11 and water vapor and likewise indicated dominance of tropospheric air in September and of stratospheric air in May in the midlatitude LMS. Our long-term measurements support these results from the campaign-based measurements.

As outlined above, CH_3Cl contains further information and in addition allows the discrimination of air of tropical and extratropical origin. Consequently, we further partition the tropospheric term in equations (2) and (3) using CH_3Cl data as follows:

$$[CH_3Cl] = \alpha_{\text{tropics}}[CH_3Cl]_{\text{tropics}} + \alpha_{\text{ex-tropics}}[CH_3Cl]_{\text{ex-tropics}} + \alpha_{\text{strat}}[CH_3Cl]_{\text{strat}} \quad (4)$$

$$\alpha_{\text{tropics}} + \alpha_{\text{ex-tropics}} + \alpha_{\text{strat}} = 1, \quad (5)$$

where the subscripts “tropics” and “ex-tropics” denote tropical UT and extratropical surface air, respectively. Using these two air mass origins, we differentiate between two transport pathways (1) quasi-isentropic transport from the tropical tropopause layer [Chen, 1995; Berthet *et al.*, 2007; Sawa *et al.*, 2008; Bönisch *et al.*, 2009] represented by α_{tropics} and (2) transport of midlatitude boundary layer air by warm conveyor belts [e.g., Stohl, 2001] and/or by deep convection over continents [e.g., Fischer *et al.*, 2003; Anderson *et al.*, 2012] represented by $\alpha_{\text{ex-tropics}}$. This concept is based on the latitudinal gradient of CH_3Cl peaking in the tropical troposphere [Yokouchi *et al.*, 2000; Umezawa *et al.*, 2014]. A similar triple mass balance approach was also examined by Hoor *et al.* [2005], who used CO data from the SPURT measurements. According to the CARIBIC data, the CH_3Cl mixing ratios in the tropical UT are taken to be 700 ppt (DJF, MAM, and JJA) or 660 ppt (SON). These values are close to the observed maxima, since we consider that such an extreme case is worthwhile as a proof of concept of the usefulness of CH_3Cl data. The CH_3Cl mixing ratios in extratropical surface air were calculated based on data at the surface site Mace Head (MHD), Ireland [Montzka *et al.*, 2011]: 545 ppt (DJF), 565 ppt (MAM), 515 ppt (JJA), or 500 ppt (SON). The CH_3Cl mixing ratio of the stratospheric reservoir is set to be 210 ppt, which was estimated by extrapolating the CH_3Cl - ΔN_2O line to $\Delta N_2O = -70$ ppb (see Figure 5b). Given the α_{trop} according to the ΔN_2O mass balance, i.e., equations (2) and (3), equations (4) and (5) can be solved for α_{tropics} and $\alpha_{\text{ex-tropics}}$.

Fractions of tropical UT air (α_{tropics}) and extratropical surface air ($\alpha_{\text{ex-tropics}}$) are shown in Figures 6m–6p and Figures 6q–6t, respectively. Note that $\alpha_{\text{tropics}} + \alpha_{\text{ex-tropics}} = \alpha_{\text{trop}}$ (i.e., the second panel from the right + the rightmost panel = the middle panel). In DJF, the α_{tropics} value is generally higher than 0.4 at the tropospheric side, but decreases going deeper in the LMS. Namely, the α_{tropics} contours follow the PV isolines, showing that the tropopause prevents the tropical UT air from being transported into the LMS. The remaining fraction is compensated by $\alpha_{\text{ex-tropics}}$, which occupies a larger fraction (>0.5) almost regardless of the tropopause location. In MAM, the α_{tropics} contours still hold the gradient following the PV isoline. In the LMS, both α_{tropics} and $\alpha_{\text{ex-tropics}}$ drop to below 0.5 and 0.4 above the 4 PVU surface, respectively. In JJA, a high tropical tongue ($\alpha_{\text{tropics}} > 0.5$) extends from the tropics into the LMS horizontally around $\Theta = 340$ K. The $\alpha_{\text{ex-tropics}}$ values appear to be higher in the lower Θ layers and very low going deeper in the LMS. In SON, the tropical tongue becomes less discernible, but the α_{tropics} stays >0.5 even above the 8 PVU isoline. In contrast, the $\alpha_{\text{ex-tropics}}$ has no distinct features with low values (<0.3) in the LMS. This clearly demonstrates that the elevated

tropospheric fraction in the LMS in this season (Figure 6l) is predominantly made up of air of tropical origin (Figure 6p). These features are in general agreement with the results by Hoor *et al.* [2005]. Using CO budget calculations with three reservoirs involved in mixing with the LMS (stratospheric overworld, tropical tropopause region, and extratropical free troposphere), they estimated that the tropical fractions in the LMS are about 0.35 and 0.55 in winter/spring and summer/autumn, respectively; our α_{tropics} values are 0.37 and 0.61 in MAM and SON, respectively, when averaged over the LMS region above 4 PVU.

As described above, the most distinct feature is the tropical tongue crossing the dynamical tropopause in summer (JJA) and its expansion in the LMS in autumn (SON). It has been suggested that the LMS is ventilated by tropospheric air isentropically transported from the tropics in summer to autumn [Chen, 1995; Hoor *et al.*, 2005; Berthet *et al.*, 2007; Sawa *et al.*, 2008; Bönisch *et al.*, 2009], which is evidenced also by the result obtained in this study. We also investigated 8 day back trajectories of individual samples [van Velthoven, 2015], which however did not indicate clear tendency of recent (<5 days) tropical origins in the summer season. This is plausible because the flushing of the LMS by the tropical tropospheric air is a persistent feature gained over longer timescales (>weeks) [Chen, 1995; Berthet *et al.*, 2007] and distributions of N₂O and CH₃Cl reflect these longer timescale phenomena. We emphasize that the tropical tongue appears only in CH₃Cl (Figure 6g), but not in N₂O (Figure 6c), which is a strong indication that CH₃Cl acts as a tracer of tropical air.

In the present mass balance analysis, we consider the tropospheric and stratospheric distributions of $\Delta\text{N}_2\text{O}$ and CH₃Cl (i.e., the different mixing ratios in different reservoirs). To evaluate uncertainties in our mass balance method, we examined sensitivity to changes of the boundary conditions.

1. The stratospheric reservoir is fixed with $[\Delta\text{N}_2\text{O}]_{\text{strat}} = -70$ ppb and $[\text{CH}_3\text{Cl}]_{\text{strat}} = 210$ ppt. As described earlier, the stratospheric boundary is estimated using the relationship between N₂O and age of air [Andrews *et al.*, 2001; Engel *et al.*, 2002] along with the age of air assumed by Bönisch *et al.* [2009]. A change of ± 10 ppb in $[\Delta\text{N}_2\text{O}]_{\text{strat}}$ (and a corresponding change of ± 60 ppt in $[\text{CH}_3\text{Cl}]_{\text{strat}}$) would on average only yield up to $\pm 3\%$ change in α_{strat} and $\pm 1\%$ change in α_{tropics} . It is also noted that the $\Delta\text{N}_2\text{O}$ distribution around the tropopause, which is characterized by relatively uniform mixing ratios below the tropopause and a sharp decrease above the tropopause, has been well investigated using an ample number of observations [Engel *et al.*, 2006; Hall *et al.*, 2007; Ishijima *et al.*, 2010; Kort *et al.*, 2011].
2. The midlatitude surface reservoir has seasonally varying CH₃Cl mixing ratios ($[\text{CH}_3\text{Cl}]_{\text{ex-tropics}}$) calculated from the data at MHD. To evaluate the variability of $[\text{CH}_3\text{Cl}]_{\text{ex-tropics}}$, we calculated average CH₃Cl mixing ratios at NOAA's other midlatitude sites in North America (Park Falls, Wisconsin, LEF; Harvard Forest, Massachusetts, HFM; and Trinidad Head, California, THD) for the respective seasons. The average CH₃Cl values were within ± 10 ppt (± 20 ppt) from the assigned values in DJF and MAM (JJA and SON). Such uncertainties could on average yield $\pm 5\%$ change in α_{tropics} .
3. The tropical UT reservoir is set with $[\text{CH}_3\text{Cl}]_{\text{tropics}} = 700$ ppt (DJF, MAM, and JJA) or 660 ppt (SON), solely relying on the CARIBIC data. The CARIBIC measurements showed values exceeding 700 ppt, but at the same time, CH₃Cl mixing ratios are highly variable along different flight routes even at similar latitudes [Umezawa *et al.*, 2014]. The HIAPER Pole-to-Pole Observations (HIPPOs) also indicate high CH₃Cl in the tropical UT over the Pacific, with values up to 600 ppt [Wofsy *et al.*, 2012]. Satellite data indicate that in the tropical UT (15°N–15°S), CH₃Cl mixing ratios stay high (~ 700 ppt) in boreal winter to spring and reach a minimum (~ 550 ppt) in late summer [Santee *et al.*, 2013]. They also illustrate geographically uneven CH₃Cl distributions in the UT likely due to the influence of biomass burning as well as of vegetation sources [Umezawa *et al.*, 2014]. Therefore, CH₃Cl mixing ratios in the tropical UT are most likely subject to substantial longitudinal variations that have not been well characterized. For instance, assuming 50 ppt lower values in $[\text{CH}_3\text{Cl}]_{\text{tropics}}$, α_{tropics} would be up to 25% higher. On the other hand, 50 ppt higher $[\text{CH}_3\text{Cl}]_{\text{tropics}}$ would result in α_{tropics} values lower by up to 10%. The choice of a single representative CH₃Cl mixing ratio for the tropical UT is therefore the largest source of uncertainty in reliably quantifying the fraction of tropical air in the LMS. More data in the tropics (in particular aircraft data) will be of help for more precise determination of a tropical representative value from a statistical viewpoint. However, it is also noted that CH₃Cl mixing ratios in the tropical UT inherently undergo large spatial and temporal variations due to uneven distribution of regional sources combined with variable strength and location of convection. Therefore, a truly representative single CH₃Cl mixing ratio can only be identified through extended efforts to investigate varying CH₃Cl distributions in neighboring areas, which may be required

for instance in studying individual tropical air intrusion events. Nevertheless, we note that CH₃Cl is a unique species among measurable gases, with strong tropical emissions and long atmospheric lifetime, and this study highlights its potential as a tracer of tropical air.

5. Conclusions

We have presented variations of CH₃Cl and ΔN₂O (deviation from the long-term trend at MLO) in the LMS measured in air samples collected by the IAGOS-CARIBIC passenger aircraft observatory during 2008–2012. Systematic decreases of CH₃Cl and ΔN₂O with potential temperature with respect to the thermal tropopause (ΔΘ_{TP}) are manifest. Vertical gradients in the LMS peak in spring as a result of wintertime strong subsidence of air from the stratospheric overworld. ΔN₂O shows seasonal variations with spring minima, which is more pronounced in the high ΔΘ_{TP} layers. CH₃Cl varies seasonally similar in phase to ΔN₂O in the high ΔΘ_{TP} bins, while a seasonal minimum in late summer is obvious below the tropopause (ΔΘ_{TP} < 0). We found significant linear relationships between ΔN₂O and CH₃Cl from winter to early summer, which are governed by mixing between deep stratospheric air and UT air. Such correlations vanish in late summer to autumn due to summertime flushing of the LMS by tropical tropospheric air. Based on the slope of CH₃Cl over ΔN₂O, we estimated the stratospheric lifetime of CH₃Cl to be 35 ± 7 years. We also presented distributions of ΔN₂O and CH₃Cl on potential temperature-equivalent latitude ($\varphi-\Theta$) coordinates. The ΔN₂O gradient followed locations of the dynamical tropopause throughout the year, plausibly reflecting age of air (fraction of deeper stratospheric air). On the other hand, the CH₃Cl isopleths horizontally extend across the dynamical tropopause in summer to autumn, indicating isentropic air transport from the tropical UT where the CH₃Cl mixing ratio is high. A mass balance approach was applied to the ΔN₂O and CH₃Cl data to partition air masses originating in the stratospheric overworld, the tropical UT and the extratropical lower troposphere. The result clearly illustrates the summertime ventilation of the LMS by tropical UT air, demonstrating that CH₃Cl can be an effective tracer of tropical air. More observations of atmospheric CH₃Cl mixing ratios in the tropics are helpful to utilize the mass balance method accurately.

Acknowledgments

We are grateful to Lufthansa Airlines for enabling the IAGOS-CARIBIC Observatory and Frankfurt Flughafen (Fraport) AG for financial support. We thank all CARIBIC team members. We acknowledge funding from the German Ministry of Education and Research (BMBF). The CARIBIC data and relevant information are available to other parties by contacting the CARIBIC coordinator (andreas.zahn@kit.edu) and on the CARIBIC website (<http://www.caribic-atmospheric.com>). We thank S. Montzka for the NOAA CH₃Cl data and J. Elkins and B. Hall for the NOAA N₂O data. We also would like to thank the three anonymous reviewers for a number of constructive comments.

References

- Anderson, J. G., D. M. Wilmoth, J. B. Smith, and D. S. Sayres (2012), Increased risk of ozone loss from convectively injected water vapor, *Science*, *337*, 835–839, doi:10.1126/science.1222978.
- Andrews, A. E., et al. (2001), Mean ages of stratospheric air derived from in situ observations of CO₂, CH₄, and N₂O, *J. Geophys. Res.*, *106*(D23), 32,295–32,314, doi:10.1029/2001JD000465.
- Appenzeller, C., J. R. Holton, and K. H. Rosenlof (1996), Seasonal variation of mass transport across the tropopause, *J. Geophys. Res.*, *101*(D10), 15,071–15,078, doi:10.1029/96JD00821.
- Assonov, S. S., C. A. M. Brenninkmeijer, T. Schuck, and T. Umezawa (2013), N₂O as a tracer of mixing stratospheric and tropospheric air based on CARIBIC data with applications for CO₂, *Atmos. Environ.*, doi:10.1016/j.atmosenv.2013.07.035.
- Baker, A. K., F. Slemr, and C. A. M. Brenninkmeijer (2010), Analysis of non-methane hydrocarbons in air samples collected aboard the CARIBIC passenger aircraft, *Atmos. Meas. Tech.*, *3*, 311–321, doi:10.5194/amt-3-311-2010.
- Berthet, G., J. G. Esler, and P. H. Haynes (2007), A Lagrangian perspective of the tropopause and the ventilation of the lowermost stratosphere, *J. Geophys. Res.*, *112*, D18102, doi:10.1029/2006JD008295.
- Bönisch, H., A. Engel, J. Curtius, T. Birner, and P. Hoor (2009), Quantifying transport into the lowermost stratosphere using simultaneous in-situ measurements of SF₆ and CO₂, *Atmos. Chem. Phys.*, *9*, 5905–5919, doi:10.5194/acp-9-5905-2009.
- Brenninkmeijer, C. A. M., et al. (2007), Civil Aircraft for the regular investigation of the atmosphere based on an instrumented container: The new CARIBIC system, *Atmos. Chem. Phys.*, *7*, 4953–4976, doi:10.5194/acp-7-4953-2007.
- Brown, A. T., C. M. Volk, M. R. Schoeberl, C. D. Boone, and P. F. Bernath (2013), Stratospheric lifetimes of CFC-12, CCl₄, CH₄, CH₃Cl and N₂O from measurements made by the Atmospheric Chemistry Experiment-Fourier Transform Spectrometer (ACE-FTS), *Atmos. Chem. Phys.*, *13*, 6921–6950, doi:10.5194/acp-13-6921-2013.
- Carpenter, L. J., S. Reimann, J. B. Burkholder, C. Clerbaux, B. D. Hall, R. Hossaini, J. C. Laube, and S. A. Yvon-Lewis (2014), Ozone-Depleting Substances (ODSs) and other gases of interest to the Montreal Protocol chap. 1, in *Scientific Assessment of Ozone Depletion: 2014, Global Ozone Res. and Monit. Project—Rep.*, vol. 55, World Meteorol. Organization, Geneva, Switzerland.
- Chen, P. (1995), Isentropic cross-tropopause mass exchange in the extratropics, *J. Geophys. Res.*, *100*(D8), 16,661–16,673, doi:10.1029/95JD01264.
- Dyroff, C., A. Zahn, E. Christner, R. Forbes, A. M. Tompkins, and P. F. J. van Velthoven (2014), Comparison of ECMWF analysis and forecast humidity data to CARIBIC upper troposphere and lower stratosphere observations, *Q. J. R. Meteorol. Soc.*, doi:10.1002/qj.2400.
- Engel, A., M. Strunk, M. Müller, H.-P. Haase, C. Poss, I. Levin, and U. Schmidt (2002), Temporal development of total chlorine in the high-latitude stratosphere based on reference distributions of mean age derived from CO₂ and SF₆, *J. Geophys. Res.*, *107*(D12), 4136, doi:10.1029/2001JD000584.
- Engel, A., et al. (2006), Highly resolved observations of trace gases in the lowermost stratosphere and upper troposphere from the Spurt project: An overview, *Atmos. Chem. Phys.*, *6*, 283–301, doi:10.5194/acp-6-283-2006.
- Fischer, H., et al. (2003), Deep convective injection of boundary layer air into the lowermost stratosphere at midlatitudes, *Atmos. Chem. Phys.*, *3*, 739–745, doi:10.5194/acp-3-739-2003.
- Gottelman, A., P. Hoor, L. L. Pan, W. J. Randel, M. I. Hegglin, and T. Birner (2011), The extratropical upper troposphere and lower stratosphere, *Rev. Geophys.*, *49*, RG3003, doi:10.1029/2011RG000355.

- Hall, B. D., G. S. Dutton, and J. W. Elkins (2007), The NOAA nitrous oxide standard scale for atmospheric observations, *J. Geophys. Res.*, *112*, D09305, doi:10.1029/2006JD007954.
- Hall, B. D., et al. (2014), Results from the International Halocarbons in Air Comparison Experiment (IHALACE), *Atmos. Meas. Tech.*, *7*, 469–490, doi:10.5194/amt-7-469-2014.
- Hegglin, M. I., and T. G. Shepherd (2007), O₃-N₂O correlations from the Atmospheric Chemistry Experiment: Revisiting a diagnostic of transport and chemistry in the stratosphere, *J. Geophys. Res.*, *112*, D19301, doi:10.1029/2006JD008281.
- Hegglin, M. I., et al. (2006), Measurements of NO, NO_y, N₂O, and O₃ during SPURT: Implications for transport and chemistry in the lowermost stratosphere, *Atmos. Chem. Phys.*, *6*, 1331–1350, doi:10.5194/acp-6-1331-2006.
- Hegglin, M. I., C. D. Boone, G. L. Manney, and K. A. Walker (2009), A global view of the extratropical tropopause transition layer from Atmospheric Chemistry Experiment Fourier Transform Spectrometer O₃, H₂O, and CO, *J. Geophys. Res.*, *114*, D00B11, doi:10.1029/2008JD009984.
- Hoerling, M. P., T. K. Schaack, and A. J. Lenzen (1991), Global objective tropopause analysis, *Mon. Weather Rev.*, *119*, 1816–1831.
- Hoor, P., H. Fischer, L. Lange, J. Lelieveld, and D. Brunner (2002), Seasonal variations of a mixing layer in the lowermost stratosphere as identified by the CO-O₃ correlation from in situ measurements, *J. Geophys. Res.*, *107*(D5), 4044, doi:10.1029/2000JD000289.
- Hoor, P., C. Gurk, D. Brunner, M. I. Hegglin, H. Wernli, and H. Fischer (2004), Seasonality and extent of extratropical TST derived from in-situ CO measurements during SPURT, *Atmos. Chem. Phys.*, *4*, 1427–1442, doi:10.5194/acp-4-1427-2004.
- Hoor, P., H. Fischer, and J. Lelieveld (2005), Tropical and extratropical tropospheric air in the lowermost stratosphere over Europe: A CO-based budget, *Geophys. Res. Lett.*, *32*, L07802, doi:10.1029/2004GL022018.
- Ishijima, K., et al. (2010), Stratospheric influence on the seasonal cycle of nitrous oxide in the troposphere as deduced from aircraft observations and model simulations, *J. Geophys. Res.*, *115*, D20308, doi:10.1029/2009JD013322.
- Kort, E. A., P. K. Patra, K. Ishijima, B. C. Daube, R. Jiménez, J. Elkins, D. Hurst, F. L. Moore, C. Sweeney, and S. C. Wofsy (2011), Tropospheric distribution and variability of N₂O: Evidence for strong tropical emissions, *Geophys. Res. Lett.*, *38*, L15806, doi:10.1029/2011GL047612.
- Laube, J. C., A. Keil, H. Böhmisch, A. Engel, T. Röckmann, C. M. Volk, and W. T. Sturges (2013), Observation-based assessment of stratospheric fractional release, lifetimes, and ozone depletion potentials of ten important source gases, *Atmos. Chem. Phys.*, *13*, 2779–2791, doi:10.5194/acp-13-2779-2013.
- Leedham Elvidge, E. C., D. E. Oram, J. C. Laube, A. K. Baker, S. A. Montzka, S. Humphrey, D. A. O'Sullivan, and C. A. M. Brenninkmeijer (2015), Increasing concentrations of dichloromethane, CH₂Cl₂, inferred from CARIBIC air samples collected 1998–2012, *Atmos. Chem. Phys.*, *15*, 1939–1958, doi:10.5194/acp-15-1939-2015.
- Lobert, J. M., W. C. Keene, J. A. Logan, and R. Yevich (1999), Global chlorine emissions from biomass burning: Reactive chlorine emissions inventory, *J. Geophys. Res.*, *104*(D7), 8373–8389, doi:10.1029/1998JD100077.
- Manney, G. L., et al. (2011), Jet characterization in the upper troposphere/lower stratosphere (UTLS): Applications to climatology and transport studies, *Atmos. Chem. Phys.*, *11*, 6115–6137, doi:10.5194/acp-11-6115-2011.
- Montzka, S. A., M. Krol, E. Dlugokencky, B. Hall, P. Jöckel, and J. Lelieveld (2011), Small interannual variability of global atmospheric hydroxyl, *Science*, *331*, 67–69, doi:10.1126/science.1197640.
- Nakazawa, T., M. Ishizawa, K. Higuchi, and N. B. A. Trivett (1997), Two curve fitting methods applied to CO₂ flask data, *Environmetrics*, *8*, 197–218, doi:10.1002/(SICI)1099-095X(199705)8:3<197::AID-ENV248>3.0.CO;2-C.
- Pan, L. L., W. J. Randel, B. L. Gary, M. J. Mahoney, and E. J. Hintsa (2004), Definitions and sharpness of the extratropical tropopause: A trace gas perspective, *J. Geophys. Res.*, *109*, D23103, doi:10.1029/2004JD004982.
- Pan, L. L., A. Kunz, C. R. Homeyer, L. A. Munchak, D. E. Kinnison, and S. Tilmes (2012), Commentary on using equivalent latitude in the upper troposphere and lower stratosphere, *Atmos. Chem. Phys.*, *12*, 9187–9199, doi:10.5194/acp-12-9187-2012.
- Plumb, R. A., and M. K. W. Ko (1992), Interrelationships between mixing ratios of long-lived stratospheric constituents, *J. Geophys. Res.*, *97*(D9), 10,145–10,156, doi:10.1029/92JD00450.
- Prinn, R., D. Cunnold, R. Rasmussen, P. Simmonds, F. Alyea, A. Crawford, P. Fraser, and R. Rosen (1990), Atmospheric emissions and trends of nitrous oxide deduced from 10 years of ALE-GAGE data, *J. Geophys. Res.*, *95*(D11), 18,369–18,385, doi:10.1029/JD095iD11p18369.
- Ravishankara, A. R., J. S. Daniel, and R. W. Portmann (2009), Nitrous oxide (N₂O): The dominant ozone-depleting substance emitted in the 21st century, *Science*, *326*, 123–125, doi:10.1126/science.1176985.
- Ray, E. A., F. L. Moore, J. W. Elkins, G. S. Dutton, D. W. Fahey, H. Vömel, S. J. Oltmans, and K. H. Rosenlof (1999), Transport into the Northern Hemisphere lowermost stratosphere revealed by in situ tracer measurements, *J. Geophys. Res.*, *104*(D21), 26,565–26,580, doi:10.1029/1999JD900323.
- Santee, M. L., N. J. Livesey, G. L. Manney, A. Lambert, and W. G. Read (2013), Methyl chloride from the Aura Microwave Limb Sounder: First global climatology and assessment of variability in the upper troposphere and stratosphere, *J. Geophys. Res. Atmos.*, *118*, 13,532–13,560, doi:10.1002/2013JD020235.
- Sawa, Y., T. Machida, and H. Matsueda (2008), Seasonal variations of CO₂ near the tropopause observed by commercial aircraft, *J. Geophys. Res.*, *113*, D23301, doi:10.1029/2008JD010568.
- Scheeren, H. A., et al. (2003), Reactive organic species in the northern extratropical lowermost stratosphere: Seasonal variability and implications for OH, *J. Geophys. Res.*, *108*(D24), 4805, doi:10.1029/2003JD003650.
- Schmidt, U., D. Knapska, and S. A. Penkett (1985), A study of the vertical distribution of methyl chloride (CH₃Cl) in the midlatitude stratosphere, *J. Atmos. Chem.*, *3*, 363–376, doi:10.1007/BF00122524.
- Schuck, T. J., C. A. M. Brenninkmeijer, F. Slemr, I. Xueref-Remy, and A. Zahn (2009), Greenhouse gas analysis of air samples collected onboard the CARIBIC passenger aircraft, *Atmos. Meas. Tech.*, *2*, 449–464, doi:10.5194/amt-2-449-2009.
- Schuck, T. J., K. Ishijima, P. K. Patra, A. K. Baker, T. Machida, H. Matsueda, Y. Sawa, T. Umezawa, C. A. M. Brenninkmeijer, and J. Lelieveld (2012), Distribution of methane in the tropical upper troposphere measured by CARIBIC and CONTRAIL aircraft, *J. Geophys. Res.*, *117*, D19304, doi:10.1029/2012JD018199.
- Solomon, S., M. Mills, L. E. Heidt, W. H. Pollock, and A. F. Tuck (1992), On the evaluation of ozone depletion potentials, *J. Geophys. Res.*, *97*(D1), 825–842, doi:10.1029/91JD02613.
- SPARC (2013), *SPARC Report on the Lifetimes of Stratospheric Ozone-Depleting Substances, Their Replacements, and Related Species*, SPARC Rep., vol. 6, edited by M. K. W. Ko et al., WCRP-15/2013. [Available at www.sparc-climate.org/publications/sparc-reports/.]
- Sprung, D., and A. Zahn (2010), Acetone in the upper troposphere/lowermost stratosphere measured by the CARIBIC passenger aircraft: Distribution, seasonal cycle, and variability, *J. Geophys. Res.*, *115*, D16301, doi:10.1029/2009JD012099.
- Stohl, A. (2001), A 1-year Lagrangian “climatology” of airstreams in the Northern Hemisphere troposphere and lowermost stratosphere, *J. Geophys. Res.*, *106*(D7), 7263–7279, doi:10.1029/2000JD900570.
- Thouert, V., J.-P. Cammas, B. Sauvage, G. Athier, R. Zbinden, P. Nédélec, P. Simon, and F. Karcher (2006), Tropopause referenced ozone climatology and inter-annual variability (1994–2003) from the MOZIC programme, *Atmos. Chem. Phys.*, *6*, 1033–1051, doi:10.5194/acp-6-1033-2006.

- Umezawa, T., A. K. Baker, D. Oram, C. Sauvage, D. O'Sullivan, A. Rauthe-Schöch, S. A. Montzka, A. Zahn, and C. A. M. Brenninkmeijer (2014), Methyl chloride in the upper troposphere observed by the CARIBIC passenger aircraft observatory: Large-scale distributions and Asian summer monsoon outflow, *J. Geophys. Res. Atmos.*, *119*, 5542–5558, doi:10.1002/2013JD021396.
- van Velthoven, P. F. J. (2015), Meteorological analysis of CARIBIC by KNMI. [Available at http://www.knmi.nl/samenw/campaign_support/CARIBIC/]
- Volk, C. M., J. W. Elkins, D. W. Fahey, G. S. Dutton, J. M. Gilligan, M. Loewenstein, J. R. Podolske, K. R. Chan, and M. R. Gunson (1997), Evaluation of source gas lifetimes from stratospheric observations, *J. Geophys. Res.*, *102*(D21), 25,543–25,564, doi:10.1029/97JD02215.
- Waugh, D. W., and T. M. Hall (2002), Age of stratospheric air: Theory, observations, and models, *Rev. Geophys.*, *40*(4), 1010, doi:10.1029/2000RG000101.
- Waugh, D. W., et al. (1997), Mixing of polar vortex air into middle latitudes as revealed by tracer-tracer scatterplots, *J. Geophys. Res.*, *102*(D11), 13,119–13,134, doi:10.1029/96JD03715.
- Werner, A., C. M. Volk, E. V. Ivanova, T. Wetter, C. Schiller, H. Schlager, and P. Konopka (2010), Quantifying transport into the Arctic lowermost stratosphere, *Atmos. Chem. Phys.*, *10*, 11,623–11,639, doi:10.5194/acp-10-11623-2010.
- Wofsy, S. C., et al. (2012), *HIPPO Combined Discrete Flask and GC Sample GHG, Halo-, Hydrocarbon Data (R_20121129)*, Carbon Dioxide Information Analysis Center, Oak Ridge Nat. Lab., Oak Ridge, Tenn. doi:10.3334/CDIAC/hippo_012(Release20121129).
- World Meteorological Organization (1957), Definition of the tropopause, *WMO Bull.*, *6*, 136.
- Yokouchi, Y., Y. Noijiri, L. A. Barrie, D. Toom-Sauntry, T. Machida, Y. Inuzuka, H. Akimoto, H.-J. Li, Y. Fujinuma, and S. Aoki (2000), A strong source of methyl chloride to the atmosphere from tropical coastal land, *Nature*, *403*, 295–298, doi:10.1038/35002049.
- Yokouchi, Y., M. Ikeda, Y. Inuzuka, and T. Yukawa (2002), Strong emission of methyl chloride from tropical plants, *Nature*, *416*, 163–165, doi:10.1038/416163a.
- Zahn, A., and C. A. M. Brenninkmeijer (2003), New directions: A chemical tropopause defined, *Atmos. Environ.*, *37*, 439–440, doi:10.1016/S1352-2310(02)00901-9.
- Zahn, A., E. Christner, P. F. J. van Velthoven, A. Rauthe-Schöch, and C. A. M. Brenninkmeijer (2014), Processes controlling H₂O in the upper troposphere/lowermost stratosphere: An analysis of eight years of monthly measurements by the IAGOS-CARIBIC observatory, *J. Geophys. Res. Atmos.*, *119*, 11,505–11,525, doi:10.1002/2014JD021687.